RNA Degradation in Cell Extracts: Real-Time Monitoring by Fluorescence Resonance Energy Transfer (FRET)

Sarah A. Uhler,† Dawen Cai,† Yunfang Man, Carina Figge, and Nils G. Walter*

Department of Chemistry, University of Michigan, Ann Arbor, Michigan 48109-1055
RECEIVED DATE (automatically inserted by publisher); nwalter@umich.edu

Supporting Information:

RNA Synthesis: All RNA oligonucleotides were obtained commercially from the HHMI Biopolymer/Keck Foundation Biotechnology Resource Laboratory RNA at the Yale University School of Medicine. RNA **1**, the stem-loop RNA, has the sequence GA(dTF)ACGUUCGCG(dTN)AUC where dTF is a fluorescein coupled to a 2'-deoxythymidine and dTN is a 2'-deoxythymidine with a 5' C6-amino linker. The unstructured RNA (RNA **2**) has the sequence GU(dTF)UCGCCAUUC(dTN)AAG, with similar modified bases. RNA oligonucleotides were deprotected and labeled as previously described.[1] The acceptor fluorophore tetramethylrhodamine was post-synthetically coupled to the amino-modifier dTN as described.[1]

Buffer Conditions: A near-physiological standard buffer was prepared containing 130 mM potassium glutamate (introducing ~100 mM K^+) and 1 mM $MgCl_2$ at pH 7.5.[2] DTT was added directly prior to experiments to a final concentration of 10 mM. Since the buffer capacity of glutamate is relatively low around physiological pH, we confirmed that the pH did not change by more than 0.1 pH units upon addition of all supplements to their highest concentration, including RNase T_1 (stored in 50 mM Tris-HCl, pH 7.5, 100 mM NaCl, 0.1 mM EDTA; then diluted in standard buffer to the appropriate concentration), protease inhibitor treated S100 cytosolic extract from HeLa cells (pH 7.6; preparation see below), and acidic aurin tricarboxylic acid (ATA; added to not higher than 0.5 mM final concentration), unless otherwise noted.

S100 Cytosolic Extract From HeLa Cells: This cell extract was a gift from Danny Reinberg (Department of Biochemistry, State University of New Jersey, Rutgers) and was prepared following published protocols.[3] Final step is an extensive dialysis against buffer D, composed of 20 mM HEPES, pH 7.9, 20% (v/v) Glycerol, 100 mM KCl, 0.2 mM EDTA, 0.5 mM DTT, 0.5 mM PMSF; we found the pH after dialysis to be 7.6.

UV Melting Curves: 1 μM unlabeled or doubly fluorophore-labeled RNA was prepared in standard buffer and degassed under vacuum. 260 nm was used as the analytical wavelength for a UV melting experiment, and the signal at 320 nm was subtracted as background. Temperatures ramped up and down from 20 ˚C to 100 ˚C at a rate of 0.2 ˚C/minute using a Beckman DU640B Spectrophotometer with High Performance Temperature Controller and Micro Auto 6 T_m cell holder. Melting temperatures were obtained using MicroCal Origin 7.0 by fitting a Gaussian distribution to the first derivative of the background-corrected 260 nm absorbance vs. temperature plot.

FRET Melting Curves: Fluorescence spectra and intensities were recorded on an Aminco-Bowman Series 2 spectrofluorimeter (Thermo Spectronic). 50 nM double-labeled RNA (200 μL total volume) was prepared in standard buffer, heat-annealed at 70 ˚C for 2 minutes and centrifuge filtered through a 0.45 μm filter. Excitation (500-650 nm) and emission scans (350-570 nm) were collected at 10 nm/s and averaged over 5 repetitions, prior and after the experiment. The cuvette was sealed with Parafilm after carefully inserting a temperature microprobe such that it did not obstruct the light path. Fluorescein was excited at 490 nm (4 nm bandwidth) and fluorescence emission over time was recorded simultaneously at the fluorescein (520 nm, 8 nm bandwidth) and tetramethylrhodamine (585 nm, 8 nm bandwidth) wavelengths for a total of >11,000 sec, by shifting the emission monochromator back and forth. Over the total timeframe, the temperature was ramped from 20 ˚C to 68 ˚C (as measured with the microprobe), at steps of 1-5 ˚C. Once a new temperature became stable for over 100 s after a ramping step, FRET ratios $Q = F_{585}/F_{520}$ were recorded for 100 s (at 1 datum/sec), averaged and normalized to the average FRET ratio at the lowest temperature, Q_0 (i.e., $(Q-Q_0)/Q_0$ was calculated). Corrected FRET ratios were then computed by subtracting the normalized FRET ratios of stem-loop RNA **1** from the corresponding normalized FRET ratios of unstructured RNA **2** to compensate for fluorescence changes not attributed to RNA melting (but rather to direct effects of temperature on the fluorophores). The melting temperature was obtained in MicroCal Origin 7.0 by fitting a Gaussian distribution to the differential of the corrected (and smoothed) FRET ratio vs. temperature plot (Supplemental Figure A).

Steady-state FRET Assays: Steady-state fluorescence spectra and intensities were recorded on an Aminco-Bowman Series 2 spectrofluorimeter, with monochromator settings as above. 50 nM double-labeled RNA substrates were prepared as for FRET melting experiments. Experiments were preformed at 37 ˚C. Excitation (500-650 nm) and emission scans (350-570 nm) were collected at 10 nm/s and averaged over 5 repetitions, prior to kinetic steady-state FRET measurements. RNase T_1 or cell extract was added ~100 s after starting a FRET time course (final volume 200 μL). Mineral oil was then added to prevent sample evaporation. Steady-state measurements were typically collected at 1 datum/sec for 3,000 sec, or longer for slow rate constants, so that the observation window was at least twice the derived time constant τ. The assay conditions (low ionic strength, 37 ˚C) are chosen such that dissociation of most decay fragments will be fast, leading to rapid breakdown of FRET upon cleavage between the fluorescein and tetramethylrhodamine fluorophores. Inhibitor studies using varying concentration of inhibitors were performed by either pre-incubating the sample with inhibitor prior to addition of enzyme, or by adding inhibitors subsequent to addition of enzyme, as indicated. A FRET ratio $Q (= F_{585}/F_{520})$ was calculated and normalized to the initial value Q_0 as above. The resulting time traces were fit to single-exponential decay functions of the form $y = y_o + A_1(1-e^{-t/\tau})$ in MicroCal Origin 7.0 to extract the rate constants $k_{dec} = \tau^{-1}$. To extract Hill parameters, the dependence of the rate constant k_{dec} on a concentration [X] was fit, using MicroCal Origin 7.0, to the Hill equation:[1]

$$k_{dec} = k_{\max} \frac{[X]^n}{[X]^n + K_M{}^n},$$

to yield an apparent affinity K_M for X and a cooperativity or Hill constant n (found to be 1, or non-cooperative).

GelFRET Analysis: GelFRET assays were performed using samples prepared as for steady-state FRET experiments, with 10 pmol FRET labeled RNA per time point. Degradation was arrested at specific times by addition of Contrad70® to a final concentration of 10% (v/v) and a of pH 9.3. Samples were diluted in an equal volume of loading buffer (80% formamide, 0.025% xylene cyanol, 0.025% bromophenol blue, 50 mM EDTA) and loaded onto a denaturing, 20% polyacrylamide, 8 M urea, gel between low-fluorescence glass plates. After electrophoresis for 1 hour at 50 V/cm, the gel was scanned in a FluorImager SI fluorescence scanner with ImageQuant software (Molecular Dynamics) as described previously.[1,4] Briefly, a laser excited fluorescein at 488 nm and the gel was scanned for fluorescence emission using a photomultiplier tube with either a 530 nm band-pass (for the donor fluorescein) or a 610 nm long-pass filter (for the acceptor tetramethylrhodamine). RNAs labeled with only fluorescein and only tetramethylrhodamine were included as color calibration standards. Defining the readout of $F_{\text{fluorescein}}$ as green and $F_{\text{tetramethylrhodamine}}$ as red, the corresponding color images were superimposed using Photoshop 7.0 (Adobe) to generate Figure 2c. A yellow band indicates fluorescence from both fluorescein and tetramethylrhodamine (upon FRET); a green band indicates fluorescein only labeled RNA, while a tetramethylrhodamine only labeled RNA is not detected. Specific cleavage products were identified by comparison with size markers generated by alkaline (cleavage 3' of every nt) and RNase T_1 (cleavage 3' of G) digestion of the same RNA.

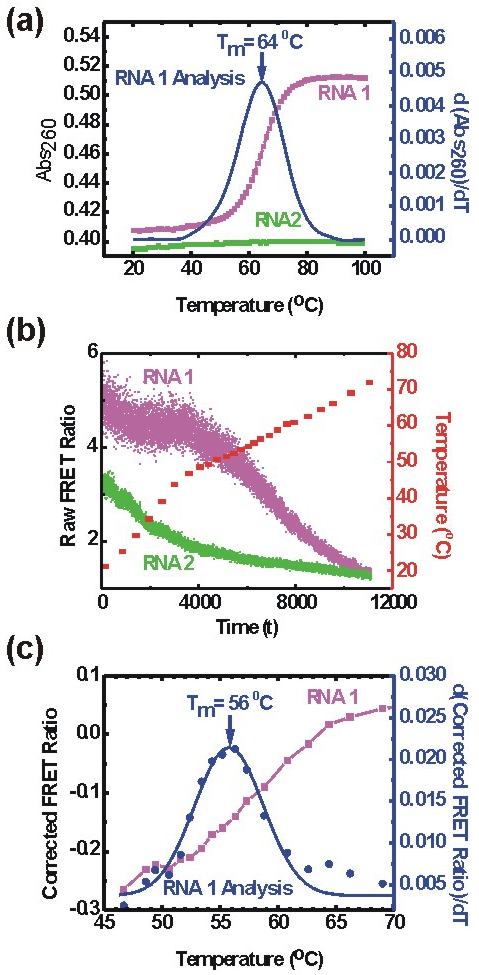

Supplemental Figure A (a) UV melting of RNA to confirm the expected secondary structures of RNAs **1** and **2**. A cooperative melting curve was obtained for RNA **1**, the first derivative of which (blue) fits a Gaussian curve that yields the indicated melting temperature T_m. RNA **2** shows no such melting transition, consistent with its lack of secondary structure. (b) Raw FRET ratios $Q = F_{585}/F_{520}$ of RNAs **1** and **2** upon temperature increase. Over the shown timeframe, the temperature was ramped from 20 ˚C to 68 ˚C, as measured in the cuvette; the red bars indicate time windows in which the given temperature had stabilized. (c) FRET melting curve. In the time windows of stable temperature, FRET ratios were recorded for 100 sec, averaged and normalized to Q at the lowest temperature. Corrected FRET ratios were then calculated by subtracting the normalized FRET ratios of stem-loop RNA **1** from the corresponding normalized FRET ratios of unstructured RNA **2** to compensate for fluorescence changes not due to RNA melting. A Gaussian distribution (blue line) was fit to the first derivative of the corrected and smoothed FRET ratios (blue dots) to yield the indicated melting temperature T_m. The results replicate those of UV melting, demonstrating the ability of FRET to monitor changes in the secondary structure of RNA **1**.

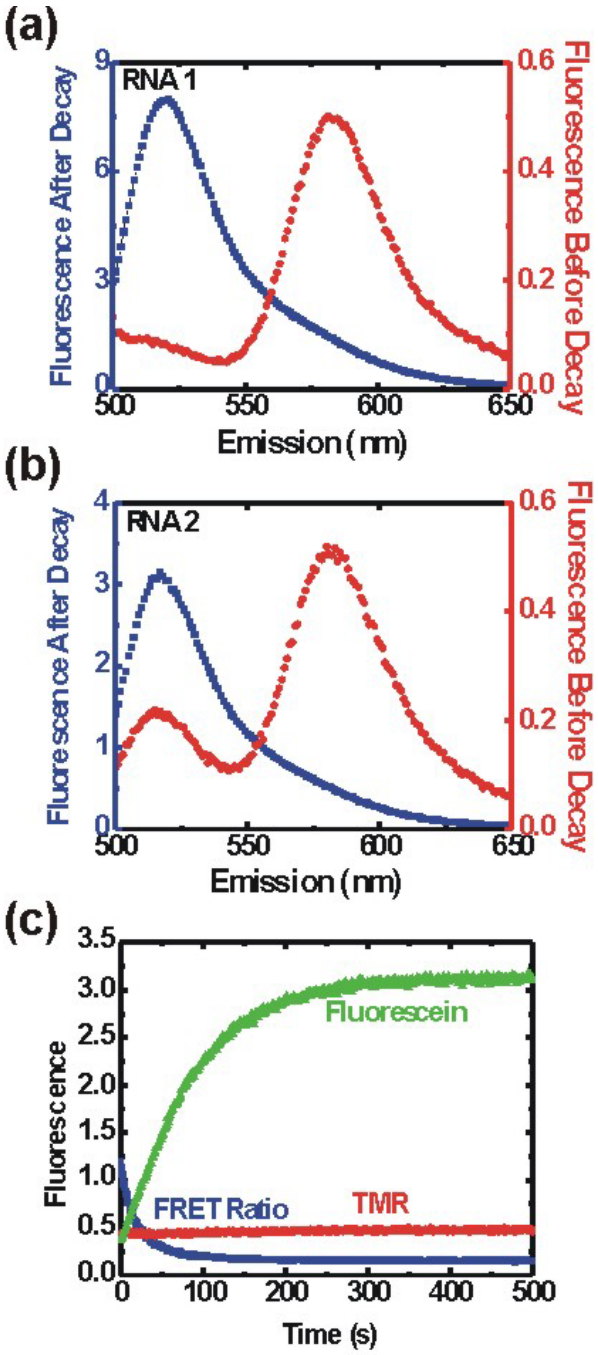

Supplemental Figure B (a) Emission spectrum of 50 nM RNA **1** before and after degradation by 75 nM RNase T_1 in standard buffer at 37 °C. (b) Emission spectrum of 50 nM RNA **2** before and after degradation by 75 nM RNase T_1 in standard buffer at 37 °C. Note that FRET (as indicated by a high 585 nm tetramethylrhodamine peak and a low 520 nm fluorescein peak) in the unstructured RNA **2** is nearly as high as in the stem-loop RNA **1**, and very much higher than in the degraded RNA samples. (c) A typical kinetic steady-state FRET assay records an increase in fluorescein emission and a concomitant decrease in tetramethylrhodamine emission over time due to cleavage of the RNA and breakdown of FRET. Shown here is the degradation of 50 nM RNA **1** by 75 nM RNase T_1 in standard buffer at 37 °C. A rate constant k_{dec} of 1.33 min^{-1} was derived by fitting a single-exponential decay curve to the FRET ratio as described above.

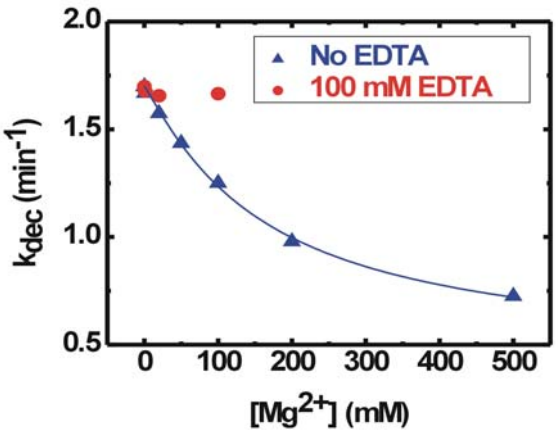

Supplemental Figure C The addition of Mg^{2+} inhibits degradation of 50 nM RNA **1** by 75 nM RNase T_1 in standard buffer at 37 °C. Preincubation with 100 mM EDTA sequesters the Mg^{2+}, thereby preventing the inhibition.

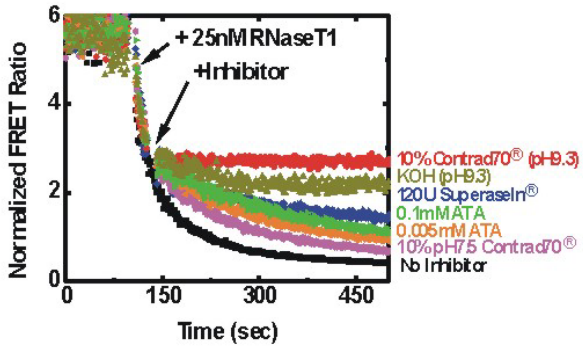

Supplemental Figure D Inhibitor studies using RNase T_1 demonstrate the varying efficacies of Contrad70® at pH 9.3 and 7.5, pH 9.3 alone (adjusted by addition of KOH), SuperaseIn®, and ATA to inhibit degradation of 50 nM RNA **1** by 25 nM RNase T_1 in standard buffer at 37 °C. Inhibition by pH 9.3 alone was reversible, while that by 10% Contrad70 at pH 9.3 was not (data not shown). Rate constants were derived by fitting single-exponential decay curves to the data as described above.

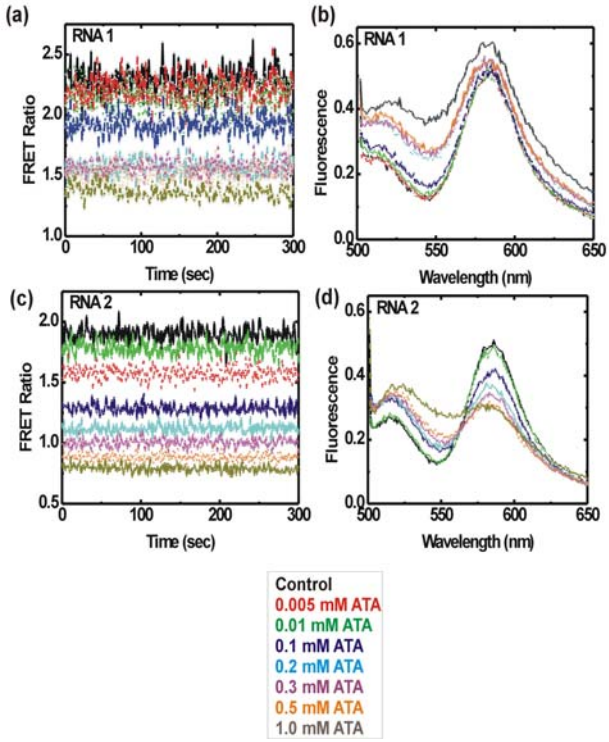

Supplemental Figure E. The RNA structure is modified by the addition of ATA, as monitored by FRET. (a) The FRET ratio for RNA **1** is stable over time but its value depends on the concentration of ATA. (b) The fluorescence emission spectrum of RNA **1** shows an increase in fluorescein emission (peak at 520 nm) in response to ATA addition, while no corresponding increase in tetramethylrhodamine emission (peak at 585 nm) is observed. This indicates either a small change in FRET efficiency or dequenching of fluorescein. (c) The FRET ratio for RNA **2** is stable over time but its value depends on the concentration of ATA. (d) The fluorescence emission spectrum of RNA **2** shows an increase in fluorescein emission (peak at 520 nm) and a corresponding decrease in tetramethylrhodamine emission (peak at 585 nm) in response to ATA addition, a clear indication of a decrease in FRET efficiency. This indicates that the unstructured RNA **2** is affected more by ATA than the stem-loop structure of RNA **1**.

References

(1) (a) Walter, N. G. *Methods* **2001**, *25*, 19-30. (b) Walter, N. G.; Harris, D. A.; Pereira, M. J.; Rueda, D. *Biopolymers* **2002**, *61*, 224-242. (c) Walter, N. G. Curr. *Protocols Nucleic Acid Chem.* **2002**, *11.10*, pp. 11.10.11-11.10.23. (d) Pereira, M. J.; Harris, D. A.; Rueda, D.; Walter, N. G. *Biochemistry* **2002**, *41*, 730-740. (e) Harris, D. A.; Rueda, D.; Walter, N. G. *Biochemistry* **2002**, *41*, 12051-12061. (f) Jeong, S.; Sefcikova, J.; Tinsley, R. A.; Rueda, D.; Walter, N. G. *Biochemistry* **2003**, in press.

(2) Christensen, K. A.; Myers, J. T.; Swanson, J. A. *J. Cell Sci.* **2002**, *115*, 599-607.

(3) Dignam, J. D.; Lebovitz, R. M.; Roeder, R. G. *Nucleic Acids Res.* **1983**, *11*, 1475-1489.

(4) Ramirez-Carrozzi, V.R.; Kerppola, V.K. *Methods* **2001**, *25*, 31-43.